Adv. Radio Sci., 10, 271–277, 2012
www.adv-radio-sci.net/10/271/2012/
doi:10.5194/ars-10-271-2012

Advances in Radio Science

Planetary wave characteristics of gravity wave modulation from 30–130 km

P. Hoffmann and Ch. Jacobi

Institute for Meteorology, University of Leipzig, Stephanstr. 3, 04103 Leipzig, Germany

Correspondence to: P. Hoffmann (phoffmann@uni-leipzig.de)

Abstract. Fast gravity waves (GW) have an important impact on the momentum transfer between the middle and upper atmosphere. Experiments with a circulation model indicate a penetration of high phase speed GW into the thermosphere as well as an indirect propagation of planetary waves by the modulation GW of momentum fluxes into the thermosphere. Planetary wave characteristics derived from middle atmosphere SABER temperatures, GW potential energy and ionospheric GPS-TEC data at midlatitudes reveal a possible correspondence of PW signatures in the middle atmosphere and ionosphere in winter around solar maximum (2002–2005). In the case of the westward propagating 16-day wave with zonal wavenumber 1 a possible connection could be found in data analysis (November–December 2003) and model simulation. Accordingly, GW with high phase speeds might play an essential role in the transfer of PW and other meteorological disturbances up to the ionospheric F-region.

1 Introduction

Ionospheric variations have a disturbing impact on GPS navigation systems and radio communication. Via the two carrier frequencies of the GPS satellites such electron density disturbances can be partly corrected and ensure the commercial application of this product. In turn ionospheric science community is interested in variability. New knowledge about characteristic of planetary wave (PW) like structures coming from the lower atmosphere are expected. For this purpose comparisons with other meteorological observations (reanalyses, satellites) will give more insight into a possible coupling (e.g. Borries et al., 2007; Borries and Hoffmann, 2010; Goncharenko et al., 2010; Hoffmann et al., 2011). It is supposed that fast small scale gravity waves (GW) excited in the troposphere are able to penetrate the thermosphere/ionosphere system and transfer momentum and also indirect properties of PW through GW modulation. This indirect signal of PW is usually identified as the PW signature (PWS). Planetary waves cannot exist in the ionospheric plasma. Dynamic features at periodicities of PW that are seen in the ionosphere therefore must be of indirect nature and forced by neutral atmosphere. Thus, they are termed as PW Type Oscillations (PWTO).

In this paper we present preliminary results from satellite data analyses of GW potential energy with respect to spectral PW characteristics and numerical model experiments by changing the spectrum of GW.

2 Planetary wave proxies

The long-term analysis of PW proxies (Borries and Hoffmann, 2010; Hoffmann et al., 2011) at midlatitudes ($\sim$50° N) from 2002 to 2008 using different data sets as stratosphere temperatures, lower thermosphere GW potential energy and ionospheric GPS-TEC maps (processed at DLR Neustrelitz, Jakowski et al., 2002), represents the seasonal behaviour of PW, PWS and PWTO (Fig. 1, left). The comparison of PW with PWTO (upper panel) and of PWS with PWTO (lower panel) indicate correspondence of wave activity between the middle and upper atmosphere. While the proxy of traveling PW activity in the stratosphere shows a less disturbed annual cycle with a maximum in winter, the PWTO variance in the ionosphere appears superposed by the solar activity at time-scales of several years (solar cycle) and of several weeks (solar rotation). However, both stratosphere and ionosphere show a maximum of wave activity during the winter season. If we look at the indirect PW signal GW potential energy, there are characteristic structures in PWS during winter 2003/04 and 2004/05 that fit quite well to the characteristics found in the ionosphere. This fact may have two causes. On the one hand, the solar rotation period may modulate GW in the lower thermosphere and, on the other hand, what we

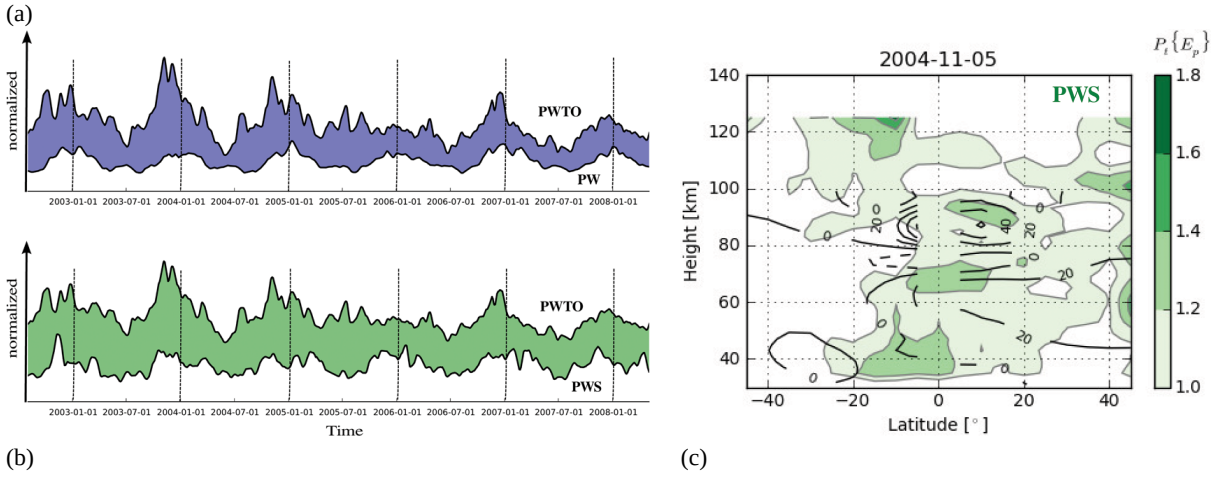

Fig. 1. Left: time series of PW proxies at midlatitudes from 2002 to 2008: stratospheric PW, ionospheric PWTO **(a)** and PWS and ionospheric PWTO **(b)**. Right: height-latitude cross section of PWS derived from SABER temperatures on 2004-11-05 **(c)**. The geostrophic zonal wind is given in black contours.

observe is the meteorological part on the total variability of the ionosphere.

The spatial structure of the GW modulation (Fig. 1, right) derived from Sounding of the Atmosphere using Broadband Emission Radiometry (SABER) data centered around 2004-11-05 indicates that PWS (green scaling) on the winter hemisphere (45° N) are able to penetrate the lower thermosphere. The vertical propagation of atmospheric GW is determined by the background wind and PW. Global wind wave disturbances lead to a periodic filtering of GW and a possible indirect transfer of PW into the ionospheric F-region. The geostrophic zonal wind component derived from SABER (black contours) indicates weak westerlies in early winter.

In order to determine the connection of PW properties in the stratosphere and ionosphere spectral components need to be considered. Furthermore, the spectrum, which in Fig. 1 is characterized by the vertical wavelength $\lambda_z < 6$ km, must be extended to longer ones ($\lambda_z = 5\ldots10$ km). These GW are faster and more likely to penetrate the thermosphere. In the following we present a method to filter GW energy from satellite temperature profiles and to analyze PW characteristics spectrally in space and time (Sect. 3). The modeling part (Sect. 4) will demonstrate the role of GW parameters in the simulation of the middle and upper atmosphere variability.

3 Planetary wave characteristics

Unevenly spaced data from the SABER instrument on board the TIMED satellite (Mertens and et al., 2004) provide temperature profiles (30–130 km) with a global coverage (50° S–50° N) since 2002. In this section we apply a space-time method (Pancheva et al., 2009) to analyze PW from temperature fields and PWS from potential energy.

3.1 GW potential energy

For the calculation of the potential energy E_p we consider single profiles $T(z)$ and apply a Savitzky-Golay filter (Savitzky and Golay, 1964) to fit the background profile $T_\mathrm{B}(z)$ (Fig. 2, left). An example of the residuals at 50.7° N, 267.1° E on 2003-12-20 are shown in the middle panel of Fig. 2. Other than on the summer hemisphere, the vertical wavelength spectrum is determined by PW, the semidiurnal tide and GW, which partly corresponds with each other. In principle, an additional horizontally filtering of global-scale waves from the background would be necessary in order to consider pure GW information (e.g. Preusse et al., 2006; Ern et al., 2011), but this is not applied here, because this method is not applicable to a running space-time analysis. Finally, the residuals are band-pass filtered and $T_\mathrm{F}(z)$ includes fluctuations in the range of $\lambda_z = 5\ldots10$ km. The Brunt-Väisälä frequency $N^2 = \frac{g}{T_\mathrm{B}}\left(\frac{\mathrm{d}T_\mathrm{B}}{\mathrm{d}z} - \Gamma\right)$ is determined, with Γ as the vertical temperature gradient and g the gravitational acceleration. The potential energy is then calculated as $E_\mathrm{p} = \frac{1}{2}\left(\frac{g}{N}\right)^2\left(\frac{T}{T_\mathrm{B}}\right)^2$ and integrated over a sliding 15 km interval. From the dispersion relation of internal GW the horizontal phase speed $c_\mathrm{ph} \backsimeq \frac{\lambda_z N}{2\pi}$ is proportional to the vertical wavelength. Consequently, fast GW have long vertical wavelength. For our configuration ($\lambda_z = 5\ldots10$ km) the phase speed is in a range of $16\ldots32\,\mathrm{m\,s^{-1}}$ with $N = 0.02\,\mathrm{s^{-1}}$.

The atmospheric background near the Equator is mainly determined by the diurnal tide. At high latitudes of the summer hemisphere only the semidiurnal component dominates because PW cannot propagate upward during easterlies. In our further considerations we focus on midlatitudes on the winter hemisphere for investigating the characteristics of PWS.

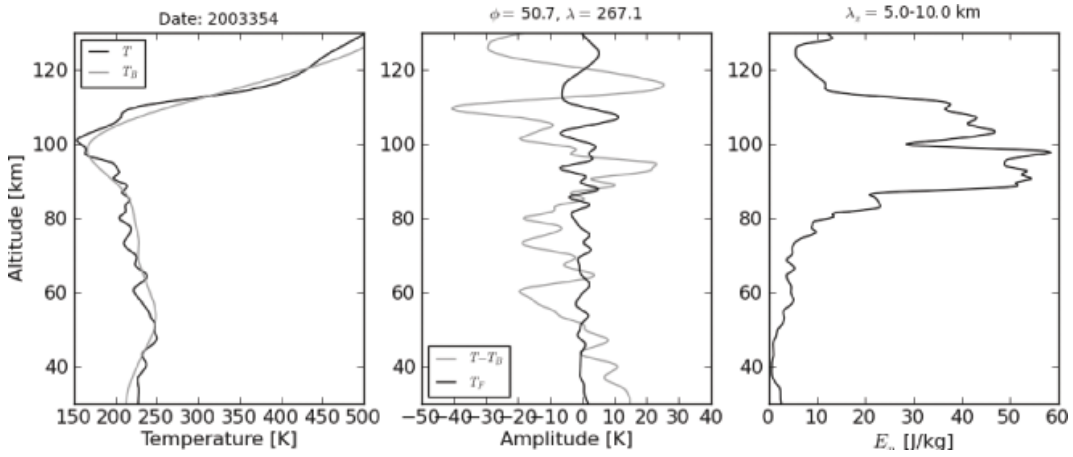

Fig. 2. Principle to derive GW potential energy E_p from SABER temperature profiles (50.7° N, 267.1° E) on the day of year 354 in 2003. Left: sounding of the temperature from 30–130 km (black line) and the fitted background (grey line); middle: residuals (grey line) and the band-pass filtered signal (black line); right: the potential energy profile for $\lambda_z = 5$–10 km.

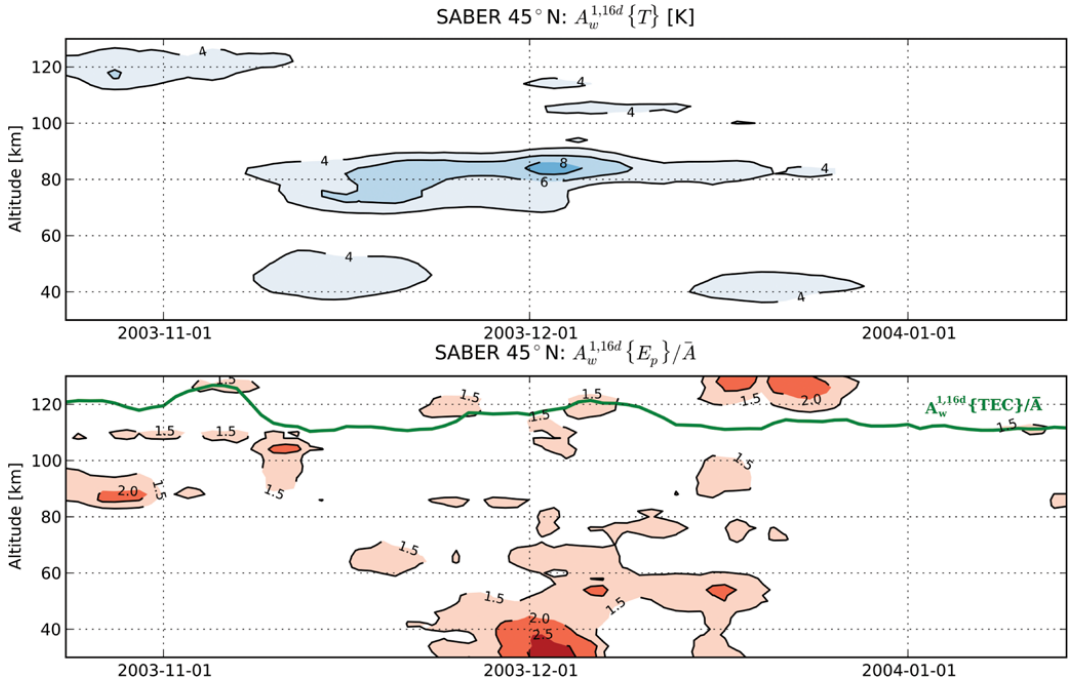

Fig. 3. Height vs. time cross section of the westward propagating 16-day wave ($k = 1$) amplitude at 45° N in temperature (top) and potential energy (bottom). The potential energy amplitudes are normalised. The course of this component derived from ionospheric GPS-TEC is shown as added (green curve).

3.2 Space-time spectral method

In this section we present results from space-time spectral analysis (Pancheva et al., 2009) of PW and PWS derived from SABER temperature and potential energy profiles in the latitude range centered around $\phi = 45° \text{ N} \pm 2.5°$ and averaged vertically over 2 km.

Because the variance analysis (Fig. 1) results in correspondences between PWS and PWTO around solar maximum, we consider the winter situation during November 2003 to February 2004. Figure 3 (top) shows the amplitude distribution of the westward propagating 16-day wave with zonal wavenumber ($k = 1$) in a height vs. time cross section. Two maxima in mid November and December at 40 km (∼4 K) and a stronger one near 80 km (∼8 K) exists.

The pattern of PW activity in the stratosphere and mesosphere changes with height. There are times when a lack of PW activity at 40 km (1 December) goes along with a strong signal at 80 km, but usually not at higher altitudes. Maybe the signals of the 16-day waves in early December above 80 km, which corresponds to the 16-day wave in the ionosphere, come from GW. These are included in the unfiltered temperature profile.

The indirect signatures of PW analyzed from GW modulation is shown in Fig. 3 (bottom). Here, the amplitudes are normalized with respect to the time average at each height. Additionally, the course of the 16-day wave in the ionospheric F-region is represented by the green line. A behaviour of PWS that is more variable and partly different from that of PW is seen. In general we observe characteristics of a long-periodic PW above 100 km in the modulation of GW energy that correspond with PWTO in the ionospheric F-region.

4 Numerical modeling

4.1 The Middle and Upper Atmosphere Model

The Middle and Upper Atmosphere Model (MUAM) is able to simulate the variability of the thermosphere (Pogoreltsev et al., 2007). Although the model does not includes the ionospheric component of the upper atmosphere an appropriate tuning of the parametrized GW will extend the application to processes that are responsible for the vertical coupling of the middle atmosphere with the thermosphere-ionosphere system. MUAM is usually forced at the lower boundary with climatological mean reanalysis fields for individual months of mean temperature cross sections (1000–30 hPa) and the first three stationary wave components in temperature as well as geopotential height at 1000 hPa. In order to study the response of the neutral upper atmosphere to changes in the GW parameters we run the GW scheme (Jacobi et al., 2006) in an offline mode.

Figure 4 depicts the simulated January mean meridional circulation (arrows) up to the F-region (∼400 km). The mean zonal wind jets (contours) dominate the dynamics of the middle atmosphere (yellow filled). Above, at thermospheric heights the ionosphere is symbolized by the blue scaling. As shown by different model experiments (e.g. Miyoshi and Fujiwara, 2008; Yiğit and Medvedev, 2010) tropospherically forced fast GW have an important impact on the thermosphere circulation and this will be also examined with MUAM.

4.2 GW parametrization and offline simulations

Gravity waves parameterized in MUAM are described in Jacobi et al. (2006). In order to operate offline experiments, atmospheric background fields, GW parameters and constants must be transferred to the routine in order to obtain GW momentum fluxes and accelerations quasi instantaneously. Here we run the scheme with doubled phase speed of GW related to the reference one characterized by phase speed ($c_{\mathrm{ph}} = [5, 10, 15, 20, 25, 30]\,\mathrm{m\,s^{-1}}$), horizontal wavelength ($\lambda_{\mathrm{h}} = 300\,\mathrm{km}$) and phase angle ($\theta = [0, 45, 90, 135, 180, 225, 270, 315]$).

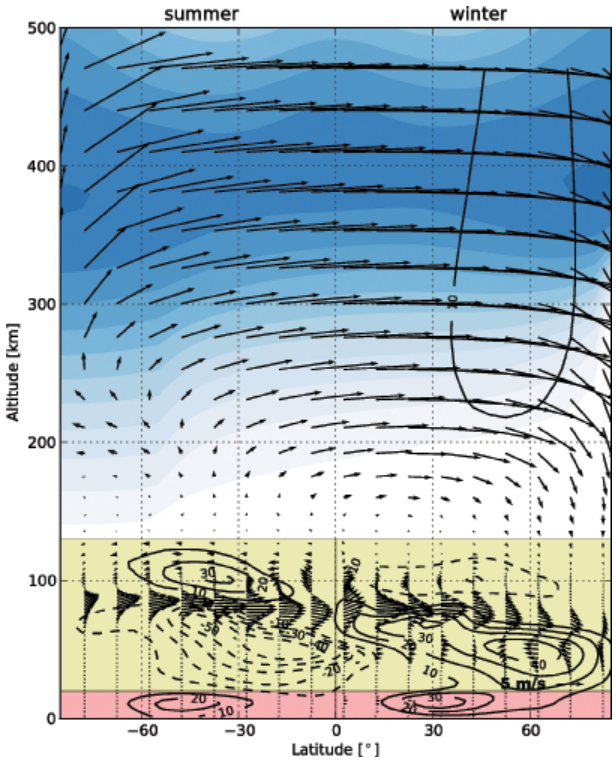

Fig. 4. Height vs. latitude cross section of the middle and upper atmosphere circulation up to the F-region height (∼400 km) simulated with MUAM for January conditions: meridional circulation (arrows), mean zonal wind (contours).

The prescribed spectrum consists of 48 different single GW with a constant horizontal wavelength. The current adjustments are tuned to the middle atmosphere in order to describe the background wind reversal in the lower thermosphere. Due to this relatively slow phase speeds of the spectrum ($\overline{c_{\mathrm{ph}}} \approx 20\,\mathrm{m\,s^{-1}}$), all GW are filtered by the mean winds and break in the upper mesosphere. No momentum fluxes are transferred into the thermosphere. Cooling and heating due to GW are calculated based on Medvedev and Klaassen (2003).

This condition changes in the case of faster GW. Yiğit and Medvedev (2010) simulated the behaviour of GW in the thermosphere with changing solar activity using TIME-GCM. The spectrum that they used has phase velocities from 2 to $80\,\mathrm{m\,s^{-1}}$. For our simulations we simply double the phase speeds that correspond to 10 to $60\,\mathrm{m\,s^{-1}}$. This corresponds to periods between 1…8 h. Figure 5 (middle panel) shows

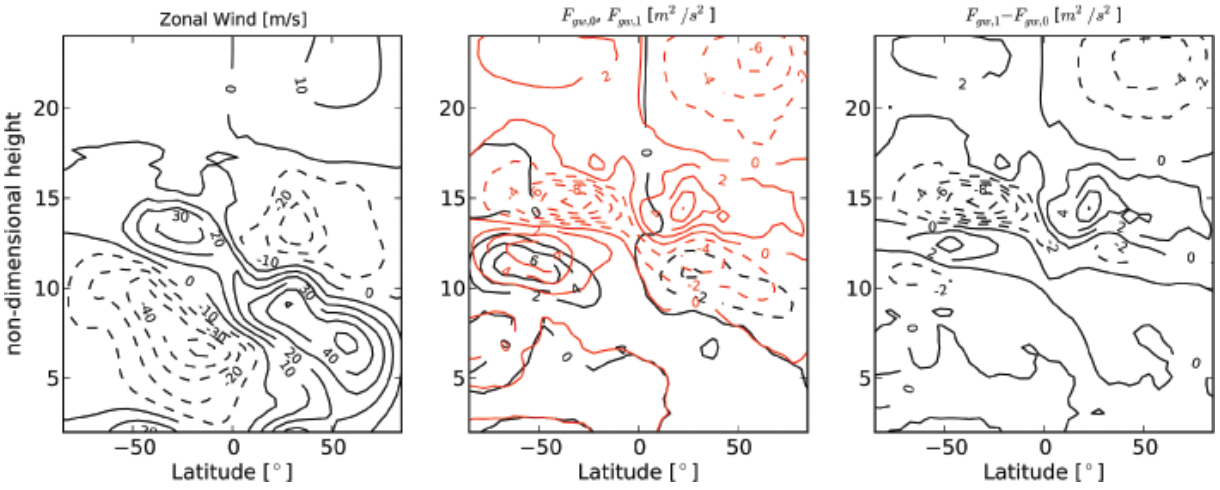

Fig. 5. Simulated atmospheric background zonal wind (left), and GW momentum fluxes (middle) for the standard phase speeds ($F_{\mathrm{GW},0}$, black) and the double phase speeds ($F_{\mathrm{GW},1}$, red). The differences pattern is given in the right panel. The non-dimensional height is defined as $x = -\ln\left(\frac{p}{p_0}\right)$ with $p_0 = 1000$ hPa ($x = 15$ about 100 gpkm).

the momentum fluxes. The comparison indicates a possible coupling between the middle and upper atmosphere by fast GW (red contours). Because small-scale GW are not only filtered by the mean wind (left panel) but also by the superposed global-scale disturbances also PW characteristics may be indirectly propagate upward in the thermosphere. This can be demonstrated by running the GW scheme offline with a modeled (non-stationary) background atmosphere.

4.3 Online simulations

A model simulation has been performed, in which the phase speeds are two times larger than in the standard configuration. Additionally, an externally forced 16-day wave, westward travelling with $k = 1$, was forced. The simulation represents January–February condition, when PW can directly propagate upward to the mesopause region (Fig. 6, colorscaling) on the Northern Hemisphere. The signatures of these PW characteristics in the modulation of GW fluxes are visible at greater altitudes. The applied analysis method is based on Pancheva et al. (2009). We show height vs. latitude cross sections of the mean (A_{m}), the stationary wave 1 (A_{s}^{1}) and the westward propagating 16-day wave ($A_{\mathrm{w}}^{1,16\mathrm{d}}$) amplitude in the temperature (T) and GW momentum flux in zonal direction (F_{GW}).

By comparing the pattern of the direct and indirect PW amplitude distribution we found an extension of the 16-day wave into the thermosphere through GW modulation (Fig. 6, right). The wave maxima are located on the Northern Hemisphere. The reason is that travelling PW in winds periodically filter momentum fluxes of fast GW. In the case of the SPW1 signature (Fig. 6, middle) the summer maximum is connected with other processes that must be also considered, e.g. interaction with tides and in situ generations through instabilities.

5 Conclusions

The combination of satellite data analysis and model simulations were presented in order to physically explain a possible coupling mechanism through GW, which are able to carry PW characteristics into the thermosphere/ionosphere system. SABER temperature data (30–130 km) have been used to analyze PW and estimate GW energy at midlatitudes. From 2002 to 2008 proxies of PW indicate a possible connection between characteristics in the GW modulation and PW type oscillations (PWTO) in the total electron content (TEC) derived from GPS during the first three winters. A more detailed spectral decomposition when the proxy indicates a positive correspondence from November 2003 to February 2004 results in first insights into the spectral characteristics of GW modulation. Amplitude maxima of the westward travelling 16-day wave in the ionospheric F-region correspond with that one of the PW signature in the lower thermosphere. In order to draw more substantial conclusions more spectral components must be considered over a longer period of time.

However, starting model experiments with faster GW (double phase velocity) that is described in the parametrization of MUAM shows, in the case of an externally forced 16-day wave, signatures in the GW momentum flux modulation between 100 and 120 km. Such a mechanism could explain part of the variability in the thermosphere/ionosphere system to the pure meteorological origin. If model simulations can be operated with an observed distribution of GW

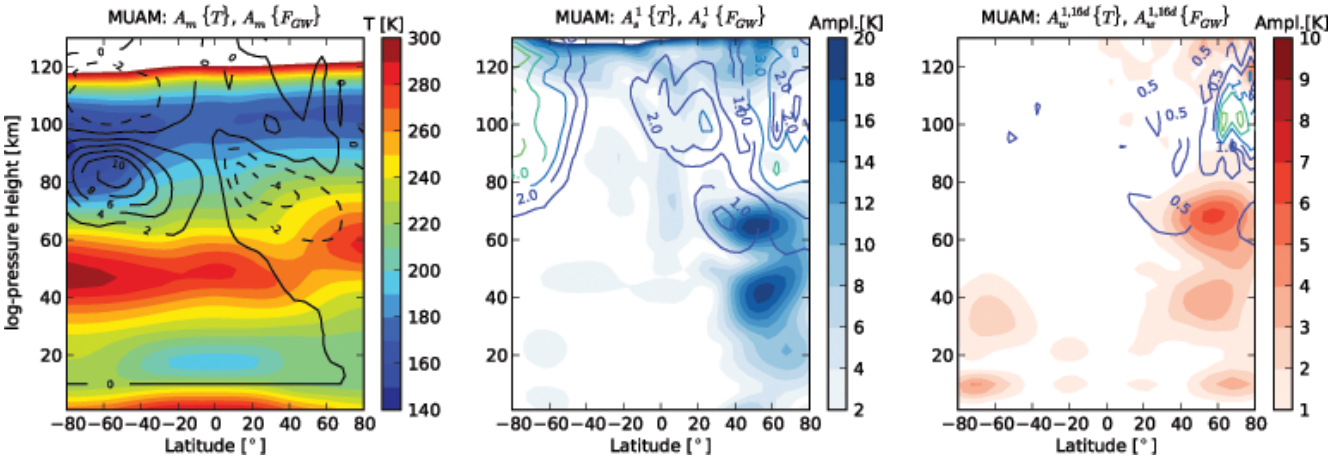

Fig. 6. Space-time spectra analysis of a MUAM simulation with double phase speeds. Shown are amplitudes in the height vs. latitude cross section. Left: mean A_m temperature (colorscaling) and GW flux (contours); middle: stationary wave 1 (A_s^1); right: westward propagating 16-day wave ($A_1^{1,16d}$).

derived from SABER using a ray-tracer model (Preusse et al., 2009) and assimilating stratospheric PW part of the resulting variability at F-region heights could be in phase with the observed ionospheric component.

Acknowledgements. We thank the SABER team for the data availability via Internet and the DLR-IKN Neustrelitz for providing the GPS-TEC data. Special thanks to the working group of A. Pogoreltsev for discussion about the potential application of MUAM. Topical Editor Matthias Förster thanks Ivan Karpov and an anonymous reviewer for their help in evaluating this paper.

References

Borries, C. and Hoffmann, P.: Characteristics of F2-layer planetary wave-type oscillations in northern middle and high latitudes during 2002 to 2008, J. Geophys. Res., 115, A00G10, doi:10.1029/2010JA015456, 2010.

Borries, C., Jakowski, N., Jacobi, C., Hoffmann, P., and Pogoreltsev, A.: Spectral analysis of planetary waves seen in the ionospheric total electron content (TEC): First results using GPS differential TEC and stratospheric reanalyses, J. Atmos. Sol.-Terr. Phy., 69, 2442–2451, doi:10.1016/j.jastp.2007.02.004, 2007.

Ern, M., Preusse, P., Gille, J. C., Hepplewhite, C. L., Mlynczak, M. G., Russell III, J. M., and Riese, M.: Implications for atmospheric dynamics derived from global observations of gravity wave momentum flux in strato- and mesosphere, J. Geophys. Res., 116, D19107, doi:10.1029/2011JD015821, 2011.

Goncharenko, L. P., Chau, J. L., Liu, H.-L., and Coster, A. J.: Unexpected connections between the stratosphere and ionosphere, Geophys. Res. Lett., 37, L10101, doi:10.1029/2010GL043125, 2010.

Hoffmann, P., Jacobi, C., and Borries, C.: A possible planetary wave coupling between the stratosphere and ionosphere by gravity wave modulation, J. Atmos. Sol.-Terr. Phy., 75–76, 71–80, doi:10.1016/j.jastp.2011.07.008, 2011.

Jacobi, C., Fröhlich, K., and Pogoreltsev, A. I.: Quasi two-day-wave modulation of gravity wave flux and consequences for planetary wave propagation in a simple circulation model, J. Atmos. Sol.-Terr. Phy., 68, 283–292, 2006.

Jakowski, N., Heise, S., Wehrenpfennig, A., Schlüter, S., and Reimer, R.: GPS/GLONASS-based TEC measurements as a contributor for space weather forecast, J. Atmos. Sol.-Terr. Phy., 64, 729–735, 2002.

Medvedev, A. S. and Klaassen, G. P.: Thermal effects of saturating gravity waves in the atmosphere, J. Geophys. Res., 108, 4040, doi:10.1029/2002JD002504, 2003.

Mertens, C. J., Schmidlin, F. J., Goldberg, R. A., Remsberg, E. E., Pesnell, W. D., Russell III, J. M., Mlynczak, M. G., López-Puertas, M., Wintersteiner, P. P., Picard, R. H., Winick, J. R., and Gordley, L. L.: SABER observations of mesospheric temperatures and comparisons with falling sphere measurements taken during the 2002 summer MaCWAVE campaign, Geophys. Res. Lett., 31, L03105, doi:10.1029/2003GL018605, 2004.

Miyoshi, Y. and Fujiwara, H.: Gravity Waves in the Thermosphere Simulated by a General Circulation Model, J. Geophys. Res., 113, D01101, doi:10.1029/2007JD008874, 2008.

Pancheva, D., Mukhtarov, P., Andonov, B., Mitchell, N. J., and Forbes, J. M.: Planetary waves observed by TIMED/SABER in coupling the stratosphere-mesosphere-lower thermosphere during the winter of 2003/2004: Part 1 – Comparison with the UKMO temperature, J. Atmos. Sol.-Terr. Phy., 71, 61–74, doi:10.1016/j.jastp.2008.09.016, 2009.

Pogoreltsev, A. I., Vlasov, A. A., Fröhlich, K., and Jacobi, C.: Planetary Waves in coupling the lower and upper atmosphere, J. Atmos. Sol.-Terr. Phy., 69, 2083–2101, 2007.

Preusse, P., Ern, M., Eckermann, S. D., Warner, C. D., Picard, R. H., Knieling, P., Krebsbach, M., Russell, J. M., Mlynczak, M. G., Mertens, C. J., and Riese, M.: Tropopause to mesopause gravity waves in August: measurement and modelling, J. Atmos. Sol.-Terr. Phy., 68, 1730–1751, 2006.

Preusse, P., Eckermann, S. D., Ern, M., Oberheide, J., Picard, R. H., Roble, R., Riese, M., Russell III, J. M., and Mlynczak,

M.: Global ray tracing simulations of the SABER gravity wave climatology, J. Geophys. Res., 114, D08126, doi:10.1029/2008JD011214, 2009.

Savitzky, A. and Golay, M. J. E.: Smoothing and Differentiation of Data by Simplified Least Squares Procedures, Anal. Chem., 36, 1627–1639, 1964.

Yiğit, E. and Medvedev, A. S.: Internal gravity waves in the thermosphere during low and high solar activity: Simulation study, J. Geophys. Res., 115, A00G02, doi:10.1029/2009JA015106, 2010.